TP = two-phase
v = vapor
W = wall
o = refers to all liquid flow

LITERATURE CITED

1. "Engineering Study of Vapor Cycle Cooling Equipment for Zero-Gravity Environment," Kymus Ginwala, ed., Wright Air Development Division *Tech. Rept. 60-776* (January, 1961).
2. Mason, J. L., W. L. Burriss, and T. J. Connolly, "Vapor-Cycle Cooling for Aircraft, Wright Air Development Center *Tech. Rept. 53-338* (October, 1953).
3. Baker, Meril, Y. S. Touloukian, and G. A. Hawkins. *Refrig. Eng.*, **61**, 986 (September, 1953).
4. Danilova, G., and J. Masewkevich, *ibid.*, **62**, 48 (December, 1954).
5. Bryan, W. L., and L. G. Siegel, *ibid.*, **63**, 361 (May, 1955).
6. Bo Pierre, *Kylteknis Tidskrift*, **16**, No. 3, p. 129, (May, 1957).
7. Bryant, W. L., and G. W. Quaint, *Refrig. Eng.*, **59**, 67 (January, 1951).
8. Corty, Claude, and Alan Foust, *Chem. Eng. Progr.*, **51**, (1955).
9. Rohsenow, W. M., *Trans. Am. Soc. Mech. Engrs.*, **74**, (July, 1952).
10. Martinelli, R. C., and D. B. Nelson, *ibid.*, **70**, 695-702 (1948).
11. Anderson, S. W., *ibid.*, **82**, 196-197 (August, 1960).
12. Rohsenow, W. M., "Heat Transfer, A Symposium, 1952," Eng. Res. Inst., Univ. Michigan, Midland, Michigan.
13. ———, and H. Y. Choi, "Heat, Mass, and Momentum Transfer," Prentice-Hall, Englewood Cliffs, New Jersey (1961).
14. McAdams, W. H., "Heat Transmission," 3 ed., McGraw-Hill, New York (1954).
15. Gilmour, C. H., *Chem. Eng. Progr.*, **54**, No. 10 (1958).
16. Chang, Y. P., unpublished material.

Manuscript received April 2, 1963; revision received November 12, 1963; Paper accepted November 14, 1963. Paper presented at A.I.Ch.E. Buffalo meeting.

Mixing on Valve Trays and in Downcomers of a Distillation Column

N. E. WELCH, L. D. DURBIN, and C. D. HOLLAND

Texas A and M University, College Station, Texas

Because of the increased use of the valve type of tray in distillation columns, this investigation was initiated. The mixing on each of two consecutive trays of a distillation column was determined. This column contained three Glitsch V-1 ballast trays. The residence-time distribution function and the eddy diffusivity were determined by means of the injection of a salt tracer followed by downstream monitoring. The output responses were correlated by use of an eddy diffusion model.

Considerable effort has been devoted to the theoretical description of mixing in flowing streams. The importance of mixing in distillation columns results from the fact that it is closely related to the plate efficiency.

Danckwerts (*6*) advanced the residence-time-distribution theory for an agitated flow system. This theory is based on the idea of an infinite number of entering streams which are destined to reside in the flow system a certain time so that a complete distribution of fluid-residence times is produced. Taylor (*17*) formulated the theory of turbulent mixing or dispersion by the cumulative effect of the action of many small eddy fluctuations. Danckwerts (*6*), Taylor (*17*), and Tichacek (*18*) developed the diffusion model for the analysis of the dispersion of a nonreacting tracer in an agitated flow process. The diffusion model is frequently approximated by the cascaded stirred-cell model. The overall dispersion in such a model is described by the choice of the proper number of perfect mixers. The similarity of the diffusion model and the cascaded stirred-cell model has been shown by Kramers and Alberda (*12*) and by Aris and Amundson (*2*). Variations of this model with recirculation and bypass streams have been discussed by Levenspiel (*14*).

In order to determine the residence-time-distribution function, dynamic methods of testing are required. Kramers and Alberda (*12*) and many other investigators have employed step function and frequency response methods. For certain boundary conditions, Levenspiel and Smith (*15*), van der Laan (*13*), Aris (*1*), and Bischoff (*4*) describe the use of the means and variances of the impulse response for the analysis of experimental results.

Recently several investigators have studied liquid mixing on distillation trays. Kirschbaum (*11*) described mixing on distillation trays by use of the cell model. Johnson and Marangozis (*10*) employed a splashing factor and the cell model in the description of the results for a single perforated plate. In the analysis of the results for bubble-cap trays, Oliver and Watson (*16*) made use of the concept of recirculation without mass transfer. Gilbert (*9*) utilized the diffusion model to interpret the frequency response results for both bubble-cap and perforated trays. The diffusion model was employed by Gerster et al. (*8*) in the analysis of the results for bubble-cap trays. Foss et al. (*7*) employed step functions in the investigation of sieve trays. Baker and Self (*3*) investigated longitudinal diffusion on a large sieve plate.

EQUIPMENT AND OPERATING PROCEDURE

The distillation column (Figure 1) employed in this investigation contained three plates that were 27 in. in diameter and were spaced 18 in. apart. A drawing of one of the plates is presented in Figure 2.

Air was blown into the column through a 5-in. line by a centrifugal blower that was capable of delivering 1,200 cu. ft. of air/min. (at standard conditions) against a head of 27 in. of water. Water was pumped into the top of the column through a 2-in. line by two centrifugal pumps, each of which was capable of delivering 180 gal./min. of water under the conditions of the experiment. Both the air and water lines were fitted with the necessary orifices and manometers required for making flow measurements. Water was recirculated though two storage tanks, each of which had a capacity of 180 gal.

External conductivity cells were attached to the downcomers of the first and second plates. In the first twenty-nine runs, the bare conductivity probes extended to the downcomer. In runs 30 through 69, the probes were located about 2 in. externally from the downcomer. In both cases liquid was withdrawn through the cells. The conductivity probes in these cells were connected to a conductivity monitor which was essentially a full wave rectifier. The conductivity monitor was connected to a d.c. source circuit in reverse bias in order to suppress the background signal for effective utilization of the full chart width. A brush recorder with two channels was used to record the conductivity signals. The data obtained are given in reference *20* and elsewhere.*

* Tabular material has been deposited as document 7919 with the American Documentation Institute, Photoduplication Service, Library of Congress, Washington 25, D. C., and may be obtained for $1.25 for photoprints or 35-mm. microfilm.

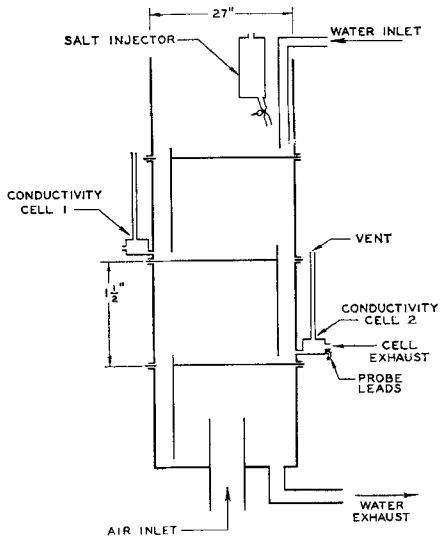

Fig. 1. Sketch of a distillation column.

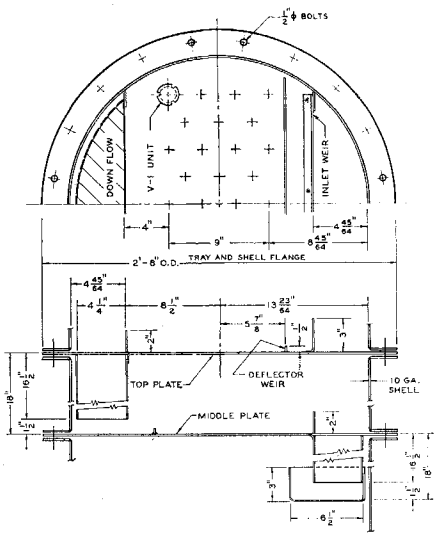

Fig. 2. Sketch of a V-1 ballast plate.

An injector was used to produce a pulse input of concentrated salt solution. This injector consisted of a steel cylinder that was provided with an air line and pressure regulator at the top and a solution line and solenoid valve at the bottom. The solenoid valve was connected with the event marker of the recorder.

To minimize mass transfer in the column, all of the equipment was isolated in a room and the experiments were performed in an environment that was nearly saturated with the solvent. The temperature of the room did not vary by more than ± 2°F. throughout the course of the investigation.

Since the recording equipment was sensitive to both humidity and to temperature, it was necessary to calibrate it at the operating conditions. Actually, the combined system (conductivity cells, conductivity monitor, d.c. bias circuit, and recorder) was calibrated against salt solutions of known concentrations as described by Welch (*20*). Also, prior to making each set of runs, certain adjustments of the equipment were made (*20*).

After the measuring and recording equipment had been properly adjusted, the solvent to be used for the given run was circulated through the column for about 20 min. in order to saturate the environment with solvent vapor and to obtain a constant temperature on each plate.

The injector (Figure 1) was first charged with a sodium chloride solution (approximately 20% by weight) and then pressurized to approximately 40 lb./sq.in. The solenoid valve of the injector was opened and closed by manipulating a switch which was also connected to the event marker of the recorder. Each injection consisted of 50 to 150 ml. of the salt solution which entered the liquid (at the position indicated in Figure 1) during a time interval that was usually about 0.2 sec. The precise time interval required for injection was indicated by the event marker of the recorder. The concentration of the salt was measured at each of two locations by conductivity cells 1 and 2. These measurements were recorded as a function of time.

The liquid mixtures consisted of water-isopropyl alcohol, water-glycerol, and water-sodium silicate whose physical properties spanned the following ranges: surface tension, 22 to 72.7 dynes/cm.; viscosity, 0.82 to 6.7 centipoise; density, 0.961 to 1.122 g./cc. Experimentation followed the same procedure as described for water except for the calibration adjustment which has been described by Welch (*20*).

The pressure drop across each plate ranged from about 2.6 to 4.5 in. of water. In the investigation of the effect of airflow rate (runs 1 through 29), air rates that ranged from 530 to 980 cu. ft./min. (at 32°F. and 1 atm.) were employed. In this range of flow rates, the ballast units were either in or almost in the fully open position. The ballast unit changed from the partially open to the fully open position in the near neighborhood of the lower flow rates employed. Liquid rates ranging from 36 to 120 gal./min. were used.

TIME-DOMAIN SOLUTION OF THE PARTIAL DIFFERENTIAL EQUATION USED TO DESCRIBE THE DIFFUSION MODEL

When the mixing on the plate of a distillation column is attributed to eddy diffusion, it can be represented by the following partial differential equation:

$$D\frac{\partial^2\Psi}{\partial x^2} - u\frac{\partial\Psi}{\partial x} = \frac{\partial\Psi}{\partial t} \qquad (1)$$

This differential equation is applicable provided the following assumptions concerning the mixing process are made.

1. The only concentration gradient existing on the plate is the one in the x-direction. This implies perfect mixing in the vertical and horizontal directions that are perpendicular to the direction of flow.
2. The departure of the outer boundaries of the plate (between the downcomers) from parallel plates (see Figure 2) is neglected.
3. The depth of liquid on the plate is taken to be the same for all values of x.

Assumptions 2 and 3 taken together imply that the cross-sectional area of the liquid is independent of x. At least two interpretations of the input signal in terms of boundary conditions exist. In the following discussions, these interpretations are presented by the use of two models. In the first model the plate is taken to be semi-infinite in length and in the second the plate is taken to be infinite.

Since all of the solutions employed contained some tap water, the flowing fluid contained a residual concentration of salt at $t = 0$ for all x. Let this concentration be denoted by $\Psi(x, 0)$. For such cases the use of Laplace transforms is facilitated by use of the function $\psi(x, t)$ defined as follows:

$$\psi(x, t) = \Psi(x, t) - \Psi(x, 0) \qquad (2)$$

Restatement of Equation (1) in terms of this function yields

$$D\frac{\partial^2\psi}{\partial x^2} - u\frac{\partial\psi}{\partial x} = \frac{\partial\psi}{\partial t} \quad (x > 0,\ t > t_o + \beta) \qquad (3)$$

To focus attention on the details of the physical process and its interpretation, the boundary conditions are stated in terms of a change in the concentration (called a pulse) of the liquid entering the system rather than in terms of the popular Dirac-delta function (*5*). At time $t = 0$, it is supposed that the given solvent is flowing at

the volumetric rate, q, across the plate, and $\psi(x, 0) = 0$. At time $t = t_o$, the concentration of the solution entering the plate at $x = 0$ is abruptly changed to a fixed value. Experimentally, this was achieved by injection of the concentrated salt solution into the liquid at the approximate position $x = 0$. This pulse is injected during the time interval from t_o to $t_o + \beta$. No further injection of the salt solution is made after time $t_o + \beta$. One interpretation of the physical process is represented by the following set of boundary conditions.

Boundary Conditions for Model I (semi-infinite plate)

(1) $\psi(x, 0) = 0 \qquad (x > 0)$

(2) $\lim_{x\to\infty} \psi(x, t) = 0$

(3a) $\psi(0, t) = 0 \qquad (t < t_o)$

(3b) $\psi(0, t) = \dfrac{A}{q\beta} \qquad (t_o < t < t_o + \beta)$

(3c) $\psi(0, t) = 0 \qquad (t > t_o + \beta)$

Boundary condition (3c) is an approximation of the actual concentration at $x = 0$. Although the injection of salt at $x = 0$ ceases at time $t_o + \beta$, it does not necessarily follow that $\psi(0, t) = 0$ for $t > t_o + \beta$. To realize this boundary condition any salt at $x = 0$ at time $t = t_o + \beta$ must be swept away immediately by the forward motion of the liquid. Because of the relatively higher velocity of the liquid passing the downcomer weir, boundary condition (3c) probably represents a good approximation.

Let $\psi(x, s)$ be the Laplace transform of $\psi(x, t)$ with respect to t. Transformation of Equation (3) and boundary conditions (2) and (3) yields

$$D\frac{d^2\psi(x,s)}{dx^2} - u\frac{d\psi(x,s)}{dx} = s\psi(x,s) \qquad (4)$$

(2) $\lim_{x\to\infty} \psi(x, s) = 0$

(3) $L\{\psi(0, t)\} = \psi(0, s)$

The solution of Equation (4) that satisfies boundary conditions (2) and (3) is

$$\psi(x, s) = \psi(0, s)\, e^{mx} =$$

$$e^{\frac{ux}{2D}}\left[\psi(0, s)\, e^{-x\sqrt{\frac{s+h}{D}}}\right] \qquad (5)$$

Since

$$L^{-1}\{\psi(0, s)\} = \psi(0, t) \text{ [defined by boundary condition (3a), (3b), (3c)]} \qquad (6)$$

$$L^{-1}\left\{e^{-x\sqrt{\frac{s+h}{D}}}\right\} = \frac{xe^{-ht - \frac{x^2}{4Dt}}}{2\sqrt{\pi D t^3}} \overset{\Delta}{=} f(t) \qquad (7)$$

the desired solution is found by the use of the convolution integral as follows:

$$\psi(x, t) = e^{\frac{ux}{2D}} \int_o^t \psi(0, \lambda)\, f(t-\lambda)\, d\lambda =$$

$$e^{\frac{ux}{2D}} \int_{t_o}^{t_o+\beta} \left(\frac{A}{q\beta}\right) f(t-\lambda)\, d\lambda \qquad (8)$$

By the mean value theorem of integral calculus

$$\psi(x, t) = \frac{A}{q} e^{\frac{ux}{2D}} f[t - (t_o + \alpha\beta)],\ 0 \leqq \alpha \leqq 1 \qquad (9)$$

The response to a perfect pulse or the impulse is defined as follows:

$$\lim_{\beta\to 0} \psi(x, t) = \lim_{\beta\to 0} \frac{A}{q} e^{\frac{ux}{2D}} f[t - (t_o + \alpha\beta)]$$

$$= \frac{A}{q} e^{\frac{ux}{2D}} f(t - t_o)$$

If time is counted from the instant just prior to the introduction of the pulse; that is, $t_o = 0^+$, the final result may be expressed as follows:

$$\psi(x, t) = \left(\frac{Ax}{2q\sqrt{\pi D t^3}}\right) e^{-\frac{(x-ut)^2}{4Dt}} \qquad (10)$$

In the correlation of the experimental results, Equation (10) was restated in the following dimensionless form

$$\phi(x, \tau) = \sqrt{\frac{N}{\pi\tau^3}}\, e^{-N\frac{(1-\tau)^2}{\tau}} \qquad (11)$$

Model II. Infinite Plate

Another interpretation of the physical process described above consists of considering the plate to be of infinite extent on each side of $x = 0$, the point at which the impulse in concentration is introduced. Also, eddy diffusion is assumed to occur freely in both directions at $x = 0$; that is, the obstruction offered by the weir to back diffusion is neglected.

The solution of this problem presented by Levenspiel and Smith (*15*) in terms of τ and N follows:

$$\phi(x, \tau) = \sqrt{\frac{N}{\pi\tau}}\, e^{-N\frac{(1-\tau)^2}{\tau}} \qquad (12)$$

It should be mentioned that in the strictest sense of the interpretation of the physical process, the partial differential equations do not apply at the underflow and overflow weirs of the downcomers. At these positions both the cross-sectional area (perpendicular to the direction of flow) and the linear velocity of the liquid differ from those on the plate.

As discussed in the next section, the data were correlated by use of both Equations (11) and (12), and both equations correlated the data equally well. Thus, at the relatively large Peclet numbers ($N = N_{Pe}/4$) employed, the approximations involved in the representation of the system by either Model I or Model II [Equations (11) and (12)] are of the same order of magnitude.

The length of the flow path used in the correlation of the data was approximate; it was measured from the point of introduction of the salt tracer to each of the monitoring positions. These lengths were taken as 3 ft. and 6 ft., respectively.

CORRELATION OF THE EXPERIMENTAL RESULTS BY USE OF THE TIME-DOMAIN SOLUTIONS

The procedure used to correlate the results by use of Equation (11) is presented. The correlation of the results by use of Equation (12) is performed in an analogous manner. In the analysis of the results, twenty-five to thirty concentrations and the respective times were taken from the output response for each run at each of the positions, namely $x = 3$ ft., $x = 6$ ft. This gave a total of about 3,500 experimental observations. In the initial analysis, an N was found by trial for each run. The best value of N for

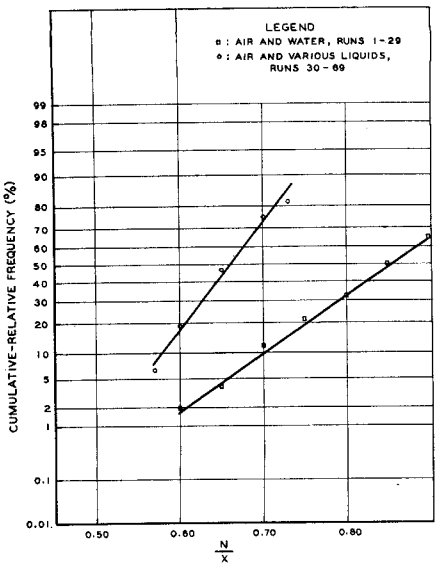

Fig. 3. The ratio N/x was independent of the gas and liquid flow rates and the physical properties of the liquid.

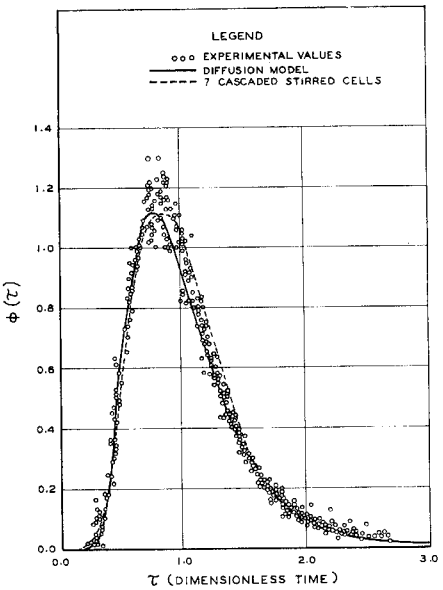

Fig. 4. Predicted output responses of the diffusion and the linear models at $x = 3$ ft.

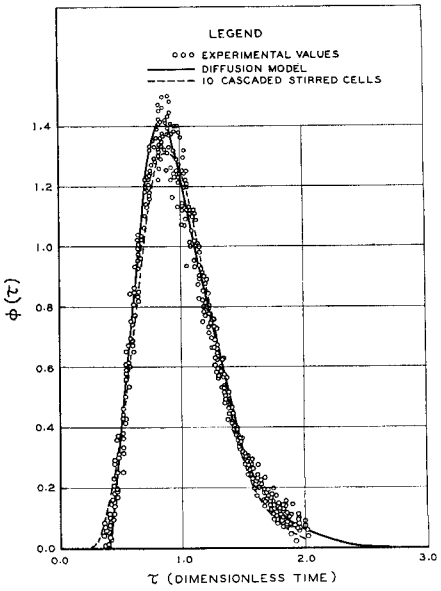

Fig. 5. Predicted output responses of the diffusion and the linear models at $x = 6$ ft.

a given run was taken as that one for which the sum of the squares of the error, ϕ(experimental—ϕ(calculated), was a minimum. The first approximation of N was calculated by use of expressions involving the mean and the mean-square times:

$$\bar{\tau} = \frac{\int_o^\infty \tau\,\phi(x,\tau)\,d\tau}{\int_o^\infty \phi(x,\tau)\,d\tau} = \left(\frac{1}{t_p}\right)\frac{\int_o^\infty t\,\psi(x,t)\,dt}{\int_o^\infty \psi(x,t)\,dt} = \frac{\bar{t}}{t_p} \tag{13}$$

$$\bar{\tau^2} = \frac{\int_o^\infty \tau^2\,\phi(x,\tau)\,d\tau}{\int_o^\infty \phi(x,\tau)\,d\tau} = \left(\frac{1}{t_p{}^2}\right)\frac{\int_o^\infty t^2\,\psi(x,t)\,dt}{\int_o^\infty \psi(x,t)\,dt} = \frac{\bar{t^2}}{t_p{}^2} \tag{14}$$

Since

$$\int_o^\infty t^n\,\psi(x,t)\,dt = (-1)^n \lim_{s\to 0}\frac{\partial^n L\{\psi(x,t)\}}{\partial s^n}$$

$$= \left[\frac{A}{q}\,e^{x\sqrt{h/D}}\,(-1)^n\right]\lim_{s\to 0}\frac{\partial^n\left(e^{-x\sqrt{\frac{s+h}{D}}}\right)}{\partial s^n} \tag{15}$$

For Model I, the integrals appearing in Equations (13) and (14) have the following values:

$$\int_o^\infty \psi(x,t)\,dt = A/q$$

$$\int_o^\infty t\,\psi(x,t)\,dt = \frac{Ax}{qu}$$

$$\int_o^\infty t^2\,\psi(x,t)\,dt = \frac{Ax^2}{qu^2}\left[1+\frac{1}{2N}\right]$$

Hence

$$\bar{t} = t_p, \bar{\tau} = 1$$

$$\bar{t^2} = (\bar{t})^2\left[1+\frac{1}{2N}\right]$$

or

$$N = \frac{1/2}{\bar{t^2}/(\bar{t})^2 - 1} = \frac{1/2}{\bar{\tau^2} - 1} \tag{16}$$

In the first twenty-nine runs (Table 1),* the liquid and air flow rates were varied. The output responses for each run were recorded as a function of time at two positions (at $x = 3$ ft. and $x = 6$ ft). The best value of N was found by a least-squares fit for each run at each of the positions. The cumulative-relative frequency of N/x was plotted vs. N/x on probability-graph paper as shown in Figure 3. Since a straight line was obtained, the variations of N/x were random; that is, the values of N/x differ because of chance rather than because of variations in the liquid and air rates.

When all of the experimental observations at $x = 3$ ft. were used simultaneously, it was found that for Model I [Equations (10) and (11), the time domain solution]

$$\frac{N}{x} = 0.85$$

This value of N was the one which minimized the sum of the squares of the deviations [ϕ (experimental) — ϕ (calculated)]. The standard deviation of the calculated values of ϕ from the experimental values was ± 0.05. At $x = 6$ ft, the following result for the first twenty-nine runs was obtained:

$$\frac{N}{x} = 0.87$$

The standard deviation of ϕ was $\cong 0.1$. For this value of N, plots of the calculated and experimental values of $\phi(x,\tau)$, as given by Equation (11) for $x = 3$ ft. and for $x = 6$ ft. vs. τ, are shown in Figures 4 and 5, respectively.

Runs 30 through 69 (Table 2)* were made to determine the effect of the physical properties (surface tension, viscosity, and density) of the liquid on N/x. Again the values of N/x at $x = 3$ ft. and at $x = 6$ ft. were determined for each run. Since a straight line was obtained when cumulative-relative frequency of occurrence of each N/x for this set of runs were plotted vs. N/x on probability-graph paper, the variations of N/x were random and not dependent on the physical properties of the liquid

* See footnote on page 373.

phase. It should be pointed out that the line for runs 30 through 69 does not coincide with the one for runs 1 through 29 because the location of the conductivity cells for the second set of runs produced a small time lag.

When the data for runs 1 through 29 were correlated on the basis of Model II [Equation (12)] the following results were obtained:

For $x = 3$ ft.

$$\frac{N}{x} = 0.87$$

For $x = 6$ ft.

$$\frac{N}{x} = 0.87$$

The standard deviations of the calculated and experimental values of ϕ for $x = 3$ ft. and $x = 6$ ft. were $\cong$ 0.05 and $\cong$ 0.1, respectively.

The good agreement of the values of N/x at $x = 3$ ft. and $x = 6$ ft. supports the use of the diffusion model for the description of mixing on plate and downcomer combinations of a distillation column. Rearrangement of the expression for N/x gives the final result

$$D \text{ (sq. ft./sec.)} = \left(\frac{x}{4N}\right) u = 0.29 \text{ (ft.) } u \text{ (ft./sec.)} \quad (17)$$

which is based on the value of $N/x = 0.86$.

USE OF THE LAPLACE AND THE FOURIER TRANSFORMS IN THE CORRELATION OF THE EXPERIMENTAL RESULTS

A combination of the Laplace and Fourier transforms may be used in two ways to correlate the data obtained in this investigation. In the first method that is described, the transforms are used to determine the best value of N for the diffusion model. In general, this approach has the advantage over the use of the solution for the time domain in that the best value of N (or D) may be determined by use of the transformed function, $\psi(x, s)$, rather than the inverted function, $\psi(x, t)$. This approach is particularly advantageous when the inversion of the transformed function is difficult to carry out.

In the second method, these transforms are used to determine an approximate linearized model for the process. This method is most useful when no simple physical theory exists for the formulation of a model.

Frequency Response

When the parameter s of the Laplace transform is allowed to take on only pure imaginary numbers ($s = j\omega$, $j = \sqrt{-1}$, and ω is a real number, the frequency in radians per second), the transfer function for frequency response is obtained. The transfer function for the diffusion model as given by Equation (5) is

$$\frac{\psi_o(j\omega)}{\psi_i(j\omega)} = e^{\frac{ux}{2D} - x\sqrt{\frac{j\omega + h}{D}}} \quad (18)$$

where for convenience

$$\psi_o(j\omega) = \psi(x, j\omega)$$

$$\psi_i(j\omega) = \psi(0, j\omega)$$

When stated in terms of the dimensionless group N and the residence time t_p, Equation (18) reduces to

$$\frac{\psi_o(j\omega)}{\psi_i(j\omega)} = e^{2N\left[1 - \sqrt{1 + \frac{jt_p\omega}{N}}\right]^{1/2}} \quad (19)$$

On the basis of the properties of the input pulse employed in this investigation, it is readily shown that

$$\frac{\psi_o(j\omega)}{\psi_i(j\omega)} = \phi(j\omega) \quad (20)$$

Thus the absolute value (or magnitude ratio) and the phase angle of the function ϕ are given by

$$|\phi(j\omega)| = e^{2N\left(1 - \sqrt{\frac{\chi}{2}}\right)} \quad (21)$$

and

$$< \phi(j\omega) = -2N\sqrt{\frac{\chi}{2} - 1} \quad (22)$$

where

$$\chi = \left[1 + \left(\frac{t_p\omega}{N}\right)^2\right]^{1/2} + 1$$

The Laplace and Fourier Transforms of a Pulse

The Laplace (or Fourier) transform of a pulse in concentration of the type employed in this investigation, namely

$$\psi(0, t) = \frac{A}{\beta q} \qquad (0 < t < \beta)$$

is given by

$$\psi_i(j\omega) = \int_0^\infty \psi(0, t)\, e^{-j\omega t}\, dt$$

$$= \frac{A}{q}\left[\frac{\sin \omega\beta}{\omega\beta} - j\frac{(1 - \cos \omega\beta)}{\omega\beta}\right] \quad (23)$$

and the magnitude of $\psi_i(j\omega)$ is

$$|\psi_i(j\omega)| = \frac{A}{q}\left[\frac{\sin\frac{\omega\beta}{2}}{\frac{\omega\beta}{2}}\right] \quad (24)$$

The perfect pulse or impulse is defined as

$$\lim_{\beta \to 0} |\psi_i(j\omega)| = \frac{A}{q}\lim_{\beta \to 0}\left[\frac{\sin\frac{\omega\beta}{2}}{\frac{\omega\beta}{2}}\right] = \frac{A}{q} \quad (25)$$

where it is, of course, understood that ω is finite. It is informative to compare the actual pulse employed in the investigation with a perfect pulse. Since β varied from about 0.15 to 0.3 sec., the actual pulse deviates most from the perfect pulse at the combination of the largest β and the largest frequency found for the system. The largest frequency was about 2 radians/sec. Thus, for the actual pulse

$$|\psi(j\omega)| = \frac{A}{q}\left[\frac{\sin\frac{(2)(0.3)}{2}}{\frac{(2)(0.3)}{2}}\right] = 0.985\frac{A}{q} \quad (26)$$

Hence, for all practical purposes the input pulse was an impulse, and Equation (23) reduces to

$$\psi_i(j\omega) = \frac{A}{q} \quad (27)$$

Numerical Evaluation of the Fourier Transform

To find N by use of either Equation (21) or (22), values for $|\phi|$ and $<\phi$ are needed. On the basis of the experimental results, values for these quantities can be obtained by means of the numerical evaluation of the Fourier transform. In this analysis it is supposed that experimental

values of $\psi(x, t)$ are known at each of several values of t for each run at each position. The details of the method of numerical integration of the function $\psi(x, t)$ have been described by Tou (*19*). In this method the abscissa (the time axis) is divided into equal increments of time, denoted by Δt. In the interval $t = n\ \Delta t - 1/2\ \Delta t$ to $t = n\Delta t + 1/2\ \Delta t$, $\psi_o(x, t)$ is approximated by its value at $t = n\ \Delta t$, namely $\psi_o(n\Delta t)$, where

$$n = 0, 1, 2, 3 \ldots$$

On the basis of these approximate values of ψ_o, the Fourier transform becomes

$$\psi_o(j\omega) = \sum_{n=0}^{\infty} \psi_o(n\Delta t) \int_{t=\left(n-\frac{1}{2}\right)\Delta t}^{t=\left(n+\frac{1}{2}\right)\Delta t} e^{-j\omega t}\, dt \qquad (28)$$

Since

$$\int_{t=\left(n-\frac{1}{2}\right)\Delta t}^{t=\left(n+\frac{1}{2}\right)\Delta t} e^{-j\omega t}\, dt = \left(\frac{\sin \frac{\omega \Delta t}{2}}{\omega/2} \right) e^{-j\omega n \Delta t}$$

Equation (28) reduces to

$$\psi_o(j\omega) = \left[\frac{\sin \frac{\omega \Delta t}{2}}{\frac{\omega \Delta t}{2}} \right] (\Delta t) \sum_{n=0}^{\infty} \psi_o(n\Delta t)\ e^{-j\omega n \Delta t} \qquad (29)$$

In view of Equation (29), it follows that

$$\frac{\psi_o(j\omega)}{\psi_i(j\omega)} = \phi(j\omega) = \left[\frac{\sin \frac{\omega \Delta t}{2}}{\frac{\omega \Delta t}{2}} \right] \left(\frac{\Delta t}{A/q} \right) \sum_{n=0}^{\infty} \psi_o(n\Delta t)\ e^{-j\omega n \Delta t} \qquad (30)$$

For each ω selected, the final result of the numerical calculational procedure may be stated as complex number

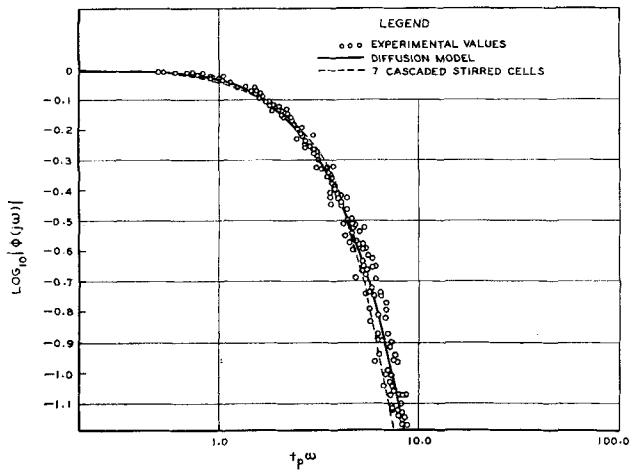

Fig. 6. Frequency response of ϕ at x = 3 ft.

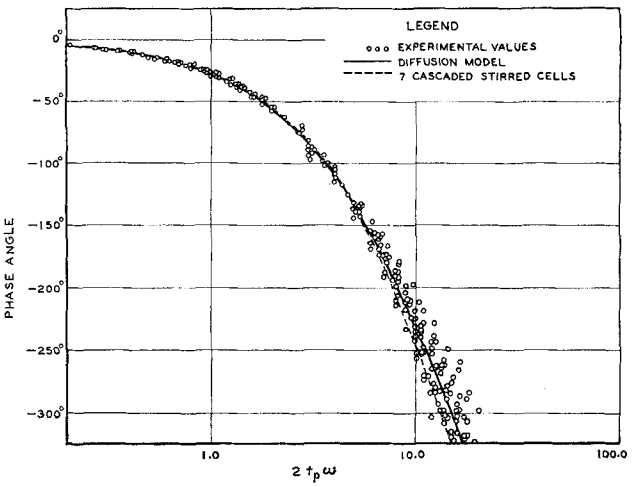

Fig. 7. Phase angle of ϕ at $x = 3$ ft.

of the form

$$\phi(j\omega) = B(\omega) + jC(\omega) \qquad (31)$$

Hence

$$|\phi(j\omega)| = \sqrt{B^2 + C^2} \qquad (32)$$

and

$$<\phi(j\omega) = \tan^{-1} C/B \qquad (33)$$

In the evaluation of B and C, a time interval of 1 sec. ($\Delta t = 1$) was used in Equation (31). It can be shown that in order to avoid frequency folding, a $\Delta t \leqq \pi/\omega_o$ should be employed (*19*). The largest value of ω (denoted by ω_o) employed in Equation (31) was 2 radians/sec. Thus the Δt employed was less than π/ω_o. At $\omega_o = 2$ radians/sec., $|\phi| \leqq 0.065$.

The data points shown in Figures 6 and 7 were obtained by the numerical evaluation of the Fourier transform of the experimental results, the time response curves. The solid lines were located by use of Equations (21) and (22) and the value of N that was found by use of the time-domain solution. Alternately, N could have been found by curve fitting the points in either Figure 6 or 7.

Approximation by a Series of Stirred Cells

Another approach to the description of mixing is to find the number of perfectly mixed cells which must be connected in series (also referred to as *cascade stirred cells*) in order to describe the experimental results shown in Figures 6 and 7. The transfer function for such a system follows:

$$\psi_o(s) = \frac{A/q}{\left(1 + \frac{\overline{t}\, s}{k}\right)^k}, \quad k > 0 \qquad (34)$$

Then, in view of Equations (20) and (27), it follows that

$$\phi(j\omega) = \frac{1}{\left(1 + \frac{\overline{t} j\omega}{k}\right)^k} \qquad (35)$$

The dimensionless form of the function in the time domain is found by taking the inverse Laplace transform of $\psi_o(s)$ and combining the obtained result with the definition of $\phi(x, \tau)$:

$$\phi(\tau) = \frac{k^k}{(k-1)!}\, \tau^{k-1}\, e^{-k\tau} \qquad (36)$$

For one plate and one downcomer, the best fit of the data was obtained by taking $k = 7$. For two plates and two downcomers, a value of $k = 10$ was required to give the best curve fit of the data. The experimental results and

the results predicted by both the series of stirred cells and the diffusion models are presented in Figures 4, 5, 6, and 7.

CONCLUSIONS

On the basis of the mechanism of eddy diffusion for turbulent mixing, the relationship, D (sq. ft./sec.) = 0.29 (ft.) u (ft./sec.) was obtained for distillation columns with ballast trays. This value can be predicted within an interval of less than 8%, 95% of the time. Also, the concentration is given by Equation (10). This relationship ($D = 0.29u$) applies when air rates are employed so that the ballast units (or valves) are in the fully open position

The mixing was found to be independent of the air flow, and the physical properties, surface tension, viscosity, and density had no significant effect on the eddy diffusivity, D.

The use of the diffusion model for the description of the mixing on a ballast tray is supported by the fact that the resulting values of N and the eddy diffusivity were correlated with good accuracy by Equation (17) as well as the fact that N/x varied less than 1% for a factor of two in position.

At lower air flow rates where the ballast units are in a partially open position, it may be found that the eddy diffusivity depends upon the air flow rate as well as the physical properties of the liquid. When air rates are employed so that the valves are open, the results show that over the range of the variables investigated the maximum degree of mixing which can be achieved by passing air through the liquid is realized regardless of the physical properties of the liquid. With regard to the separation of the mixing on the plate and in the downcomer, it is anticipated that the value of the concentration at the outlet weir as computed by Equation (10) would be conservative.

ACKNOWLEDGMENT

This work was supported by the Fritz W. Glitsch & Sons, Inc. and the Texas Engineering Experiment Station. This aid is gratefully acknowledged.

NOTATION

A = pounds of salt contained in the input pulse, lb.

B, C = function of the ω used in Equation (31), dimensionless

D = eddy diffusivity; sq. ft./sec.

e = base for natural (or Naperian) logarithms

$f(t)$ = a function of time used in the development, defined by Equation (7)

h = $u^2/4D$, 1/sec.

j = $\sqrt{-1}$

m = $\dfrac{u}{2D} - \sqrt{\dfrac{s+h}{D}}$

n = a counting integer, 0, 1, 2, 3, . . .

N = $\dfrac{ux}{4D} = N_{Pe}/4$, where N_{Pe} is the Peclet number, dimensionless

q = volumetric flow rate of the liquid, cu. ft./sec.

s = a parameter appearing in the Laplace transform of a function with respect to time

S = cross-sectional area of the liquid in the direction of flow, sq. ft.

t = time, sec.

t_o = particular time the salt was injected into the liquid, sec.

t_p = residence time; length of the flow path divided by the mean velocity of the liquid; $t_p = x/u$, sec.

$\overline{t}$ = mean time, defined by Equation (13), sec.

$\overline{t^2}$ = mean-square time, defined by the Equation (14); sec.^{2}

Δt = increment of time used in the numerical evaluation of the Fourier transform of the time-response data, sec.

u = mean-linear velocity of the liquid across the plate, ft./sec.

x = distance traveled by the liquid; measured from the point of injection of the pulse of salt tracer, ft.

Greek Letters

β = period of time required to inject the pulse of salt solution into the system, sec.

λ = dummy variable in the convolution integral, Equation (8), sec.

π = 3.1416 radians

τ = dimensionless time; $\tau = t/t_p$

$\overline{\tau}$ = mean-dimensionless time, defined by Equation (13)

$\overline{\tau^2}$ = mean-square-dimensionless time, defined by Equation (14)

$\phi(x, \tau)$ = $\dfrac{t_p\,\psi(x,\tau)}{A/q}$, the dimensionless concentration function at the point of measurement

χ = a function of t_p, ω, and N; defined after Equation (22), dimensionless

ψ = concentration of the salt in the solvent at any x above that contained by the solvent before the injection of the pulse, lb./cu. ft.

ψ_i = value of ψ at $x = 0$ during the time period β

ψ_o = output value of ψ at any x and t

Ψ = total concentration of salt in the solvent at any x, lb./cu. ft.

ω = frequency, radians per sec; ω_o = the largest value of ω employed in the numerical integration

LITERATURE CITED

1. Aris, Rutherford, *Chem. Eng. Sci.*, **10**, 80 (1959).
2. ———, and N. R. Amundson, *A.I.Ch.E. Journal*, **3**, 280 (1957).
3. Barker, P. E., and M. F. Self, *Chem. Eng. Sci.*, **17**, 541 (1962).
4. Bischoff, K. B., *ibid.*, **12**, 69 (1960).
5. Churchill, R. V., "Operational Mathematics," 2 ed., McGraw-Hill, New York (1958).
6. Danckwerts, P. V., *Chem. Eng. Sci.*, **2**, 1 (1953).
7. Foss, A. S., J. A. Gerster, and R. L. Pigford, *A.I.Ch.E. Journal*, **4**, 231 (1958).
8. Gerster, J. A., A. B. Hill, N. N. Hochgraf, and D. G. Robinson, "Tray Efficiencies in Distillation Columns, Final Report of University of Delaware," Am. Inst. Chem. Engrs., New York (1958).
9. Gilbert, T. J., *Chem. Eng. Sci.*, **10**, 243 (1959).
10. Johnson, A. I., and J. Marangozis, *Can. J. Chem. Engrs.*, **36**, 161 (1958).
11. Kirschbaum, Emich, "Distillation and Rectification," Chemical Publishing Co., New York (1948).
12. Kramers, Ir. H., and G. Alberda, *Chem. Eng. Sci.*, **2**, 173 (1953).
13. Laan, E. Th., van der, *ibid.*, **1**, 187 (1958).
14. Levenspiel, Octave, "Chemical Reaction Engineering," Wiley, New York (1962).
15. ———, and W. K. Smith, *Chem. Eng. Sci.*, **6**, 227 (1957).
16. Oliver, E. D., and C. C. Watson, *A.I.Ch.E. Journal*, **2**, 18 (1956); **5**, 564 (1959).
17. Taylor, G. I., *Proc. Roy. Soc.*, **A219**, 189 (1953); **A225**, 473 (1954).
18. Tichacek, L. J., C. H. Barkelew, and Thomas Baron, *A.I.Ch.E. Journal*, **3**, 439 (1957).
19. Tou, J. T., "Digital and Sampled Data Control Systems," McGraw-Hill, New York (1959).
20. Welch, N. E., dissertation, Texas A and M University, College Station, Texas (1963).

Manuscript received July 1, 1963; revision received October 5, 1963; paper accepted October 10, 1963.